

# Numerical Analysis for Effect of Envelop Color of Oil Tank Storage with Floating Roof

Andisheh Tavakoli<sup>1</sup>, Mohamadreza Baktash<sup>2</sup>

<sup>1</sup>Department of Material Engineering, Amirkabir University of Technology, Tehran, Iran  
Petropars Ltd. Company, Client of Oil and Gas Project

<sup>2</sup>Department of Mechanic Engineering, K.N.Toosi University of Technology, Tehran, Iran  
Namvaran Company, Consultant of Oil and Gas Project

**Abstract:** The aim of the present work is to determine the evaporation rates from external floating storage tanks and to study the effects of their exterior surface paint on the losses due to the solar irradiation. In this study a numerical scheme has been developed for estimating the time variations of the storage tank temperature and evaporative losses. Considering this fact that the evaporation happens in the fluid surface and the surface temperature is important parameter in this process, investigate the solution for the reducing surface temperature lead to reducing evaporation. One of the methods for reducing surface temperature is reducing effect of solar radiation on the storage tank and for this aim in this study investigated effect of paint color on the evaporation loss. The results show that the absorptivity of the exterior surface paint has considerable effects on tank temperature variations and the evaporative losses accordingly. The value of annual evaporation loss for light color has 170 barrel and for dark color has 370 barrel, in order to difference of evaporation loss between good and bad paint color has 200 barrel. Note that this difference has for one crude oil storage tank and there are about 40 storage tank in Khark Island. Furthermore, the numerical value of monthly averaged evaporation losses have been compared with the estimations based on the API AP-42 standard and good agreement has been observed.

**Key words:** Storage tank; External floating roof; Evaporative losses; surface Paint; Solar radiation.

## I. INTRODUCTION

Design of storage tanks depends on various parameters such as the vapor pressure, storage temperature and pressure, and the toxicity of liquid [1]. The fixing-roof tanks are mainly used for petroleum materials with a vapor pressure less than 1.5 psia [2], while floating-roof tanks are used for petroleum materials with a vapor pressure of 1.12–11.5 psia [1]. An external floating roof tank typically consists of an open topped cylindrical steel shell equipped with a roof that floats on the surface of the storage liquid, which rises and falls as the liquid level changes. Floating roof tanks are equipped with a sealing system, which is attached to the roof perimeter and covers the gap between the roof and the tank wall [3]. The basic designs available for external floating roof rim seals are mechanical shoe seals, liquid-mounted seals, and vapor-mounted that called primary seals [4]. A secondary seal is often used for covering the entire primary seal. The floating roof structure and the sealing system are designed to reduce evaporative losses of the petroleum materials. Evaporative losses from the external floating roof tanks are limited to the losses from the sealing system and roof fittings and any remaining liquids on the tank walls, while the floating roof falls down.

There have been very limited studies related to the storage tank evaporative losses. Wongwises et al. [5] evaluated the gasoline evaporation losses from Thailand storage sites and service stations during refueling and loading. They estimated the total gasoline evaporative losses of about 21,000 tons/year throughout the Thailand. Ramachandran [3], also, investigated the underlying causes of storage tank emissions and analyzed the options of reducing them. Asharif and Zorgani [6] calculated evaporative losses from existing large crude oil storage tanks located in a Libyan oil field and investigated the operating variables including the number of separation stages, operating temperature and pressure of each separator. They concluded that the operation variables of the existing process facilities can be adjusted in order to minimize the losses from storage tanks. Digrado and Thorp [7] compared the evaporation losses between the internal and external floating roofs. They also determined the losses associated with different sealing arrangements based on the American Petroleum Institute (API) standards [8, 9]. Zareie et al. [10] experimentally determined the amount of the volatile organic compounds emitted from an industrial external floating roof tank by monitoring the level of the liquid in the tank and its temperature for a period of 35 days. They also compared their findings with the values computed based on the API standards and found out that the API predictions are slightly lower than the experimental data.

This brief review of the related literature indicates the shortage of information in the field of storage tank evaporative losses. Furthermore, the above mentioned studies are mainly focused on the general estimation of the losses. However, in the present paper a numerical method has been developed for solving the energy equation to predict the storage tank temperature and to estimate the evaporative losses. More importantly, the solar irradiation and the effects of the tank surface paint absorptivity on the tank temperature and the evaporative losses have been investigated.

## II. THE CASE STUDY

The problem under consideration is a typical storage tank in Khark Island shown in Figure 1. As seen, the exterior surface paint of the tank is white with two small rings of blue and yellow color indicating that the tank is suitable for storing both heavy and light crude oil.



Figure 1- The oil storage tank under consideration in Khark Island

The tank is an external pontoon floating roof type with 114 meters in diameter and 17 meters in height with the storage capacity of 1 million barrels of crude oil. The types and the numbers of deck fittings are listed in table 1.

Fitting Type	Construction Details	Number
Access hatch	Bolted cover, gasketed	3
Vacuum breaker	Weighted mechanical actuation, gasketed	14
Roof drain	100% open	5
Unslotted Guide Pole	Ungasketed sliding cover	2
Deck leg	Adjustable, pontoon area - gasketed	301
Rim vent	Weighted mechanical actuation, gasketed	13
Rim-seal	Primary	Liquid-mounted seal
	Secondary	Weather shield

Table 1- fitting types of the tank



Figure 2- The deck leg of tank



Figure 3- The vacuum breaker of tank

Two fitting types of the tank are shown in Figures 2 and 3. Fig 2 show deck leg of tank, the exiting of crude oil vapor from gasketed area case to blacked the near area of gasketed, figure also show exposed liquid on the tank internal walls that vaporize as time goes on. In Fig 3 show vacuum breaker. The evaporation loss from this part lead to dirty around it, also the exiting of vapor could see in shadow of vacuum breaker. During the current study light crude oil with API of 33.36 has been stored in the tank.

### III. THE NUMERICAL METHOD

The solar radiation is the main cause of the evaporative losses in the floating roof tanks. Theoretically, the solar radiation striking the earth atmosphere brings about 1.5 kW per square meter, when measured normal to the sun rays. This incident radiation is partly reflected and scattered and partly absorbed by the atmosphere [11]. For estimating solar radiation on the earth surface several engineering models have been proposed [12]. In all of the models the weather condition and geographic location are important factors. Kamali and Moradi [13] have examined various models including Angstrom, Bristow and Campbell, Hargreaves and Reddy for locations and weather conditions relevant to the present problem and compared their finding with the experimental data. It was suggested that Angstrom model with some modifications is more suitable for Khark Island conditions, and thus has also been adopted for the present study.

Based on the Angstrom model, solar radiation,  $H$ , can be estimated using the following equation:

$$\frac{H}{H_o} = a + b \frac{S}{S_o} \tag{1}$$

Where  $a$  and  $b$  are coefficients that must be chosen according to the location and weather conditions,  $S$  and  $S_o$ , are average sunshine duration and cloudless sunshine duration, respectively. Following Kamali and Moradi [13],  $a$  and  $b$  for Khark Island shown in table 3.

Table 2 – Coefficients that adjusted for Khark Island from Angstrom model

coefficient	spring	summer	autumn	winter
$a$	0.37	0.37	0.37	0.37
$b$	0.35	0.35	0.38	0.38

The cloudless hourly global irradiation received can be calculated using the following equation:

$$H_o = \frac{24 \times 3600}{\pi} \cdot I_{sc} \left( \frac{\bar{d}}{d} \right)^2 \left[ \cos \phi \cdot \cos \delta \cdot (\sin \omega_2 - \sin \omega_1) + \frac{2\pi(\omega_2 - \omega_1)}{360} \cdot \sin \phi \cdot \sin \delta \right] \tag{2}$$

Where  $I_{sc}$  is set to 1367 W/m<sup>2</sup> according to the world radiation center [13] and  $\omega$  is given by the following equation:

$$\omega = (t - 12) \times 15 \tag{3}$$

Figs. 4 and 5 show the time variations of the solar radiation,  $H$ , throughout the 5<sup>th</sup> day of each month in spring-summer and autumn-winter months throughout the year 2010, respectively. The solar radiation usually exists between 5:30 am to 18:30 pm with the pick around noon. Figures also show that the largest solar radiation occurs in June.

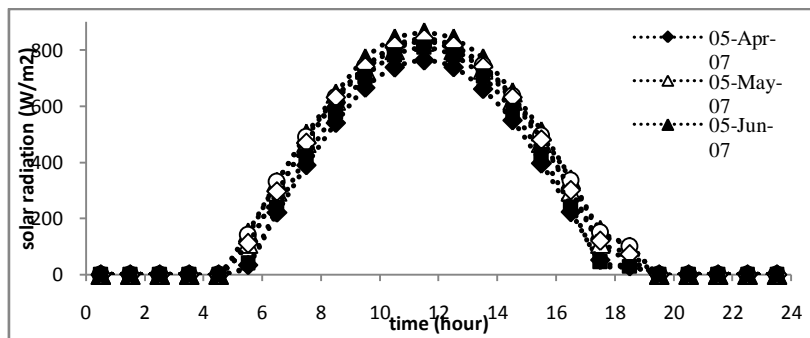


Figure 4 - Time variations of solar radiation in spring and summer months for Khark Island

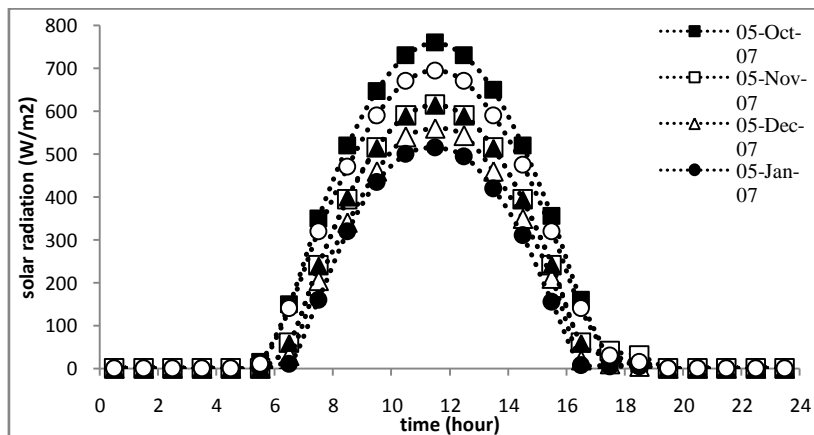


Figure 5- Time variations of solar radiation in autumn and winter months for Khark Island

A schematic diagram of the crude oil storage tank with all incoming and outgoing forms of energy is shown in Fig. 6. In developing the energy balance of the tank, the oil temperature variation inside the tank is neglected and a lumped system with uniform temperature is considered.

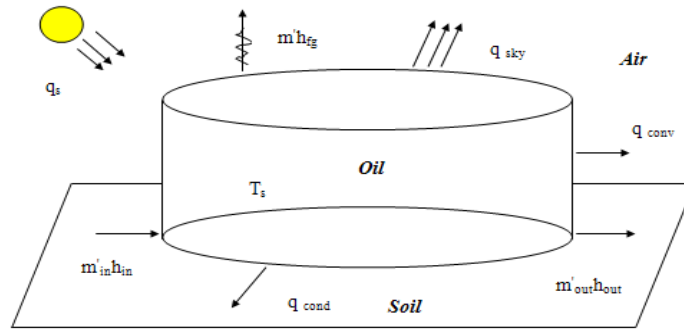


Figure 6 - Schematic of oil storage tank with all incoming and outgoing energies

Considering the tank as an open system, the energy equation can be expressed as:

$$\dot{Q} - \dot{W} + \dot{m}_{in} h_{in} - \dot{m}_{out} h_{out} - \dot{m} h_{fg} = \frac{dU}{dt} \quad (4)$$

Where  $\dot{Q}$  includes all incoming and outgoing heat fluxes expressed as:

$$\dot{Q} = q_s - q_{cond} - q_{conv} - q_{sky} \quad (5)$$

Where  $q_s$  is the absorbed solar energy by the tank surface with absorption coefficient,  $\alpha$ , and irradiating surface area of  $A_s$  with solar radiation,  $H$ , defined as:

$$q_s = \alpha \times A_s \times H \quad (6)$$

$q_{cond}$  is the amount of heat conducted to the foundation ground evaluated by Fourier's law of heat conduction:

$$q_{cond} = -k A_b \frac{dT}{dx} = k A_b \frac{T_{soil} - T_s}{\Delta x} \quad (7)$$

Where  $\Delta x$ ,  $k$ , and  $T_{soil}$  are thickness, conductivity coefficient and temperature of foundation base with the area of  $A_b$ , respectively.

$q_{conv}$  evaluates the convective exchange of energy between the tank and the ambient with temperature  $T_\infty$ :

$$q_{conv} = h A_s (T_s - T_\infty) \quad (8)$$

There are many correlations available for calculating the convective heat transfer coefficient,  $h$ , in the above equation. In this study the correlation proposed by Churchill and Bernstein [14] has been employed, which is valid for vertical cylinders, when  $RePr > 0.2$  related to the present case and expressed as:

$$\bar{Nu}_D = 0.3 + \frac{0.62 Re_D^{0.5} \cdot Pr^{1/3}}{\left[1 + \left(\frac{0.4}{Pr}\right)^{2/3}\right]^{1/4}} \cdot \left[1 + \left(\frac{Re_D}{282000}\right)^{5/8}\right]^{4/5} \quad (9)$$

Radiation heat exchange between the sky and the tank can be obtained according to:

$$q_{sky} = \sigma \cdot \epsilon \cdot A_s \cdot (T_s^4 - T_{sky}^4) \quad (10)$$

Where  $T_{sky}$  is the sky temperature evaluated following Kamali and Moradi [13] as:

$$T_{sky} = 0.0552 \times T_\infty^{1.5} \quad (11)$$

It is further assumed that the inflow and outflow rates of the crude oil are almost equal and therefore, the work done by the ambient pressure due to the negligible displacement of the tank roof related to the evaporative losses is neglected. Furthermore, the inflow enthalpy is assumed almost equal to the outflow enthalpy due to the small temperature differences. This assumption is also supported by the three dimensional numerical flow simulations inside the tank, which indicate that a large portion of the mass inflow to the tank directly moves toward the outflow region and does not mix considerably with the stored liquid, therefore:

$$\dot{W} = 0 \quad \text{and} \quad \dot{m}_{in} \dot{h}_{in} = \dot{m}_{out} \dot{h}_{out} \quad (12)$$

The time variation of the internal energy of the tank is expressed as:

$$\frac{dU}{dt} = \frac{d}{dt} (m \cdot c_p T_s) = \dot{m} \cdot c_p T_s + m \cdot c_p \cdot \frac{dT_s}{dt} \quad (13)$$

For simplicity, the quasi steady state condition has been assumed for the temperature time variation, which leads to:

$$\frac{dT_s}{dt} = 0 \quad \rightarrow \quad \frac{d}{dt} (m \cdot c_p T_s) = \dot{m} \cdot c_p T_s \quad (14)$$

The specific heat,  $c_p$ , of the crude oil is assumed to be a function of temperature as will be discussed later. The final form of the energy balance is obtained by substituting the above mentioned relations for each term in the energy equation (4) as follow:

$$\alpha HA_S + kA_b \frac{T_{soil} - T_S}{\Delta x} - hA_S(T_S - T_\infty) - \alpha \varepsilon A_s (T_S^4 - T_{sky}^4) - \dot{m} h_{fg} = \dot{m} c_p T_S \quad (15)$$

Based on the crude oil chemical composition as listed in Table 2 and with the use of HYSYS software, the following relations have been developed for the temperature dependence of evaporation enthalpy and specific heat:

$$h_{fg} = 1910T_S - 2773000 \quad (16)$$

$$c_p = 4.348T_S - 635.2 \quad (17)$$

Assuming  $T_{soil} = T_\infty$  and incorporating  $h_{fg}$  and  $c_p$  in the energy equation yields:

$$\alpha \varepsilon A_s T_S^4 + 4.348 \dot{m} T_S^2 + (1910 \dot{m} + hA_S + \frac{kA_b}{\Delta x} + 635.2 \dot{m}) \times T_S - (\alpha HA_S + kA_b \frac{T_\infty}{\Delta x} + hA_S T_\infty + \alpha \varepsilon A_s T_{sky}^4 + 2773000 \dot{m}) = 0 \quad (18)$$

The storage tank temperature,  $T_S$ , and the crude oil evaporation rate,  $\dot{m}$ , are the two unknowns of the equation. Therefore, another equation is required to close up the problem. An equation will be developed for the evaporation rate following the API method as will be discussed in the next section. Evaporative losses from the external floating roof design are limited to losses from the seal system and roof fittings (standing storage loss) and any exposed liquid on the tank walls (withdrawal loss) [4, 5]. According to the API standards [15, 16], the total rates of evaporative losses from external floating roof tanks are equal to the sum of the rim seal losses, withdrawal losses, and deck fitting losses:

$$\dot{m} = \dot{m}_R + \dot{m}_{WD} + \dot{m}_F \quad (19)$$

Rim seal loss from floating roof tanks can be estimated using the following equation:

$$\dot{m}_R = 2.5 \times 10^{-8} \times (k_{Ra} + k_{Rb} V^n) DP^* M_V K_C \quad (20)$$

Where  $K_C$  is a product factor and for crude oil is set to 0.4, while  $K_{Ra}$ ,  $K_{Rb}$ , and  $n$  are related to the used seal type. The vapor pressure,  $P^*$ , is evaluated according to:

$$P^* = \frac{\frac{P_{VA}}{P_A}}{\left[ 1 + \left( 1 - \frac{P_{VA}}{P_A} \right)^{0.5} \right]^2} \quad (21)$$

Where the true vapor pressure,  $P_{VA}$ , for selected petroleum at the stored liquid surface temperature can be determined using the following equation:

$$P_{VA} = 6.895 \times \exp \left[ A - \left( \frac{B}{T_S} \right) \right] \quad (22)$$

The constants  $A$  and  $B$  can be calculated from the following equations:

$$\begin{cases} A = 12.82 - 0.9672 \ln(RVP) \\ B = 7261 - 1216 \times \ln(RVP) \end{cases} \quad (23)$$

Where RVP is crude oil property, which is determined experimentally (given in Table 2). Deck fitting losses from floating roof tanks can be estimated according to:

$$\dot{m}_R = 2.5 \times 10^{-8} F_F P^* M_V K_C \quad (24)$$

The value of  $F_F$  is calculated using the actual tank-specific data for the number of each fit type ( $N_{Fi}$ ) multiplying by the fitting loss factor for each fitting ( $K_{Fi}$ ).

$$F_F = [(N_{F1} K_{F1}) + (N_{F2} K_{F2}) + \dots + (N_{Fn} K_{Fn})] \quad (25)$$

The deck fitting loss factor,  $K_{Fi}$  for a particular type of fitting, can be estimated by the following equation:

$$K_{Fi} = K_{Fai} + K_{Fbi} (K_V V)^{mi} \quad (26)$$

For external floating roof tanks, the fitting wind speed correction factor,  $K_v$ , is equal to 0.7. The withdrawal losses from floating roof storage tanks can be estimated using the following:

$$\dot{m}_{WD} = 2.829 \times 10^{-7} \times \frac{QC_s W_L}{D} \left[ 1 + \frac{N_C F_C}{D} \right] \quad (27)$$

Where  $N_C$  is zero for the external floating roof.

Finally, total rate of evaporative losses from external floating roof tanks can be calculated as:

$$\dot{m} = 2.5 \times 10^{-8} [F_F + D(k_{Ra} + k_{Rb} V^n)] P^* M_V K_C + 2.829 \times 10^{-7} \frac{Q C_s W_L}{D} \quad (28)$$

The vapor pressure function can be simplified by combining Equation (21) with Equation (22). The result is following equation:

$$P^* = 4 \times 10^{-7} \times e^{0.043 T_s} \quad (29)$$

Therefore, the total rate of evaporation losses can be estimated according to:

$$\dot{m} = 2.829 \times 10^{-7} \frac{Q C_s W_L}{D} + [F_F + D(k_{Ra} + k_{Rb} V^n)] M_V K_C \times 10^{-14} \times e^{0.043 T_s} \quad (30)$$

In the above equation, the evaporative rate,  $\dot{m}$ , is given as a function of the tank temperature. All other terms are constant coefficients which are determined based on the problem specifications according to the API method.

Equation 30 along with the energy balance, equation 18, is adequate to determine the tank temperature and the evaporative losses. Yet, an iterative method of trial and error is required to solve the set of equations. Consistent with the current color of the tank paint, the absorptivity of the tank is assumed to be 0.1 and 0.9 in calculation respectively.

It worth mentioning that in API method [15, 16], a simple correlation has been proposed for computing monthly averaged tank temperature, which can also be used for estimating the monthly averaged evaporative losses:

$$T_s = T_\infty + 1.86\alpha + 5 \times 10^{-5} \alpha H - 0.31 \quad (31)$$

#### IV. RESULTS AND DISCUSSION

As the first step in the evaluation of the evaporative losses, it is required to examine the accuracy of the developed numerical scheme for the tank temperature estimation. For this matter, the calculated monthly based averaged tank temperatures have been compared with their corresponding values from the API correlation given by equation 31, in Figure 7. Considering the approximate nature of both methods the results compare fairly well with each other. It must be emphasized that it is only the numerical method that provides a proper base for the study of the absorptivity of the paint effects on the transient tank temperature.

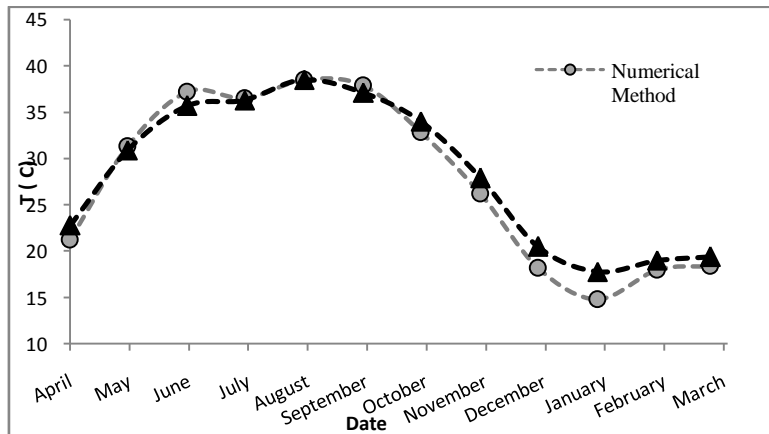


Figure 7 – Comparison between API and numerical method of monthly average tank temperature

Employing the numerical method discussed earlier the hourly variations of tank temperature have been plotted in Figs. 8 and 9 just for the 5<sup>th</sup> day of the spring and summer months, respectively. The corresponding ambient temperature variations have also been presented by dashed lines for comparison. Clearly, the tank temperature at the early and the late hours of the day is lower than the ambient temperature, which can be attributed to the exchange of radiative heat between the tank and sky with much lower value than the ambient temperature. As the sun rises, the solar radiation increases and so does the absorbed heat by the tank surface, which leads to the temperature rise of the tank. It must be emphasized that the tank temperature is also influenced by the wind speed, which can even outweigh the solar radiation. This fact is clear from Fig. 12, which shows that the highest tank temperature occurs at about noon in September, while the solar radiation is largest in June. This is due to fact that wind speed is much lower in September as compared to June.



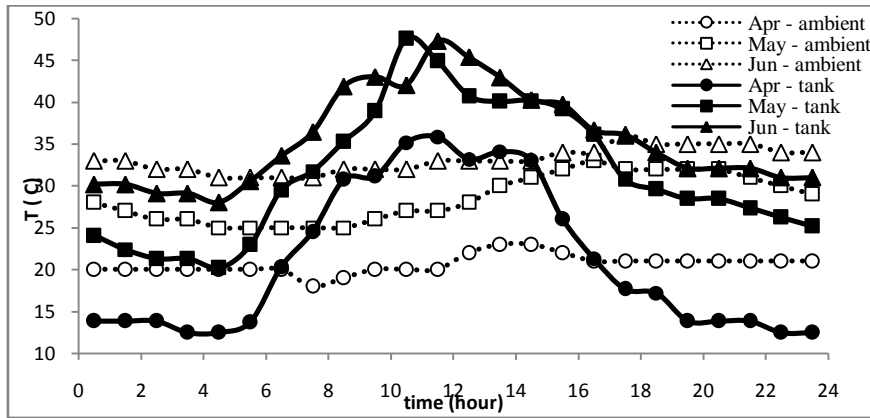


Figure 8 – Variation of the tank and ambient temperature against time in spring

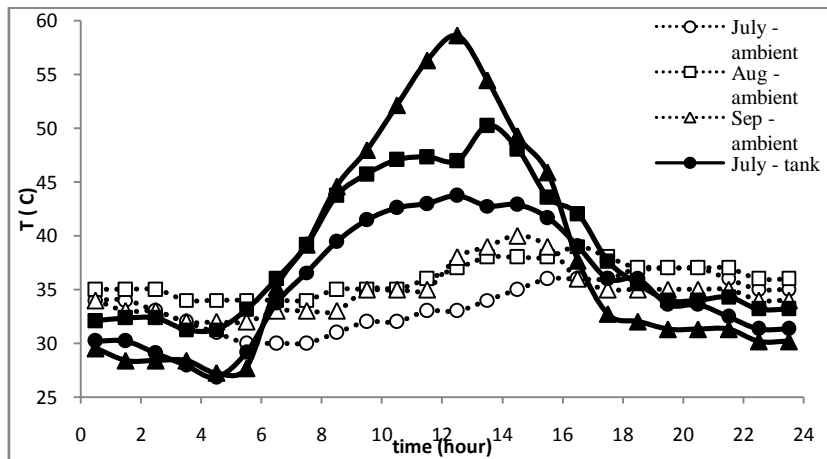


Figure 9 - Variation of the tank and ambient temperature against time in summer

Trough the developed numerical scheme the effects of the surface tank paint absorptivity on the tank temperature can be investigated, which enables the designer to select the appropriate paint that best suits the desired application. Fig. 10 shows the effects of paint absorptivity on time variations of the tank temperature during the 5<sup>th</sup> day of August 2010. It can be realized that absorptivity has strong effects on the tank temperature. The tank temperature can increase to about 40°C above the ambient temperature around 13:30 pm, when absorptivity increases from 0.1 to 0.9. Fig. 11 also shows the effects of the paint absorptivity but on the monthly averaged tank temperature. Similar to the time variation of the tank temperature the monthly averaged tank temperature can be increased by about 35°C in September, when absorptivity increases from 0.1 to 0.9.

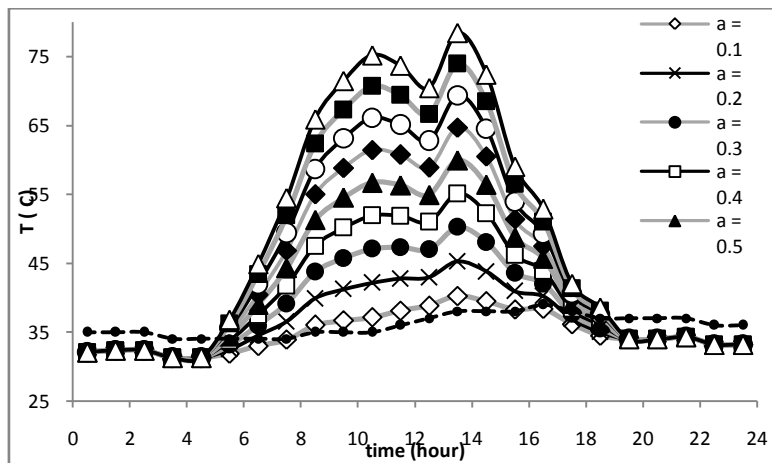


Figure 10 –Effects of absorptivity on time variations of the storage tank temperature for August 5<sup>th</sup> 2010

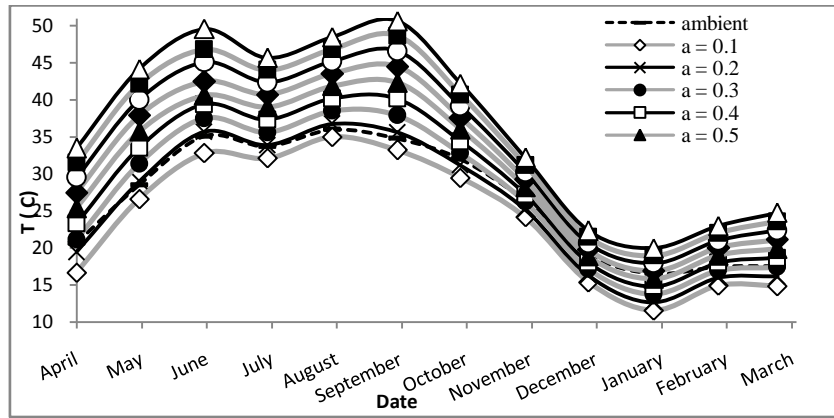


Figure 11 – Surface paint absorptivity effects on the variations of the monthly averaged tank temperature

Having examined the storage tank temperature, the evaporative losses from storage tanks can now be determined by the numerical method discussed earlier. In Fig. 12 the time variations of the evaporative losses during the 5 August 2010 are presented. The effects of the surface paint absorptivity of the storage tank on the evaporative losses can also be examined by the developed numerical method. Fig. 12 shows the effect of absorptivity of the storage tank paint on the evaporation rate from the tank during the 5<sup>th</sup> day of August 2010. It is clear that absorptivity dramatically affects the evaporation rate. An increase of about 0.18 bbl is observed, when absorptivity of the paint increases from 0.1 to 0.9.

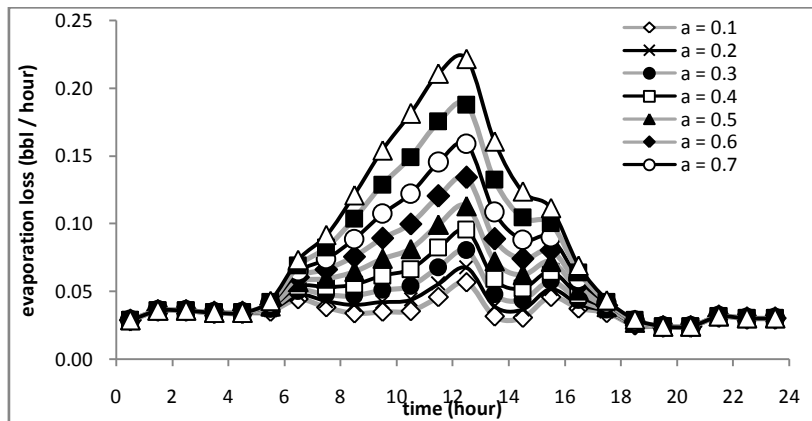


Figure 12 – Surface paint absorptivity effects on time variations of the storage tank temperature for August 5<sup>th</sup> 2010

Fig. 13 shows the variations of the monthly averaged evaporative losses from the storage tank throughout the year 2010. A comparison has also been made with the results obtained from the API method. It is expected to see that the highest evaporative losses are occurred during June, July and August, the hottest months in Khark Island. However, the local peaks in evaporative losses during October and November are due to the high wind speeds in these months. Furthermore, reasonable agreements between the results of the two methods are observed.

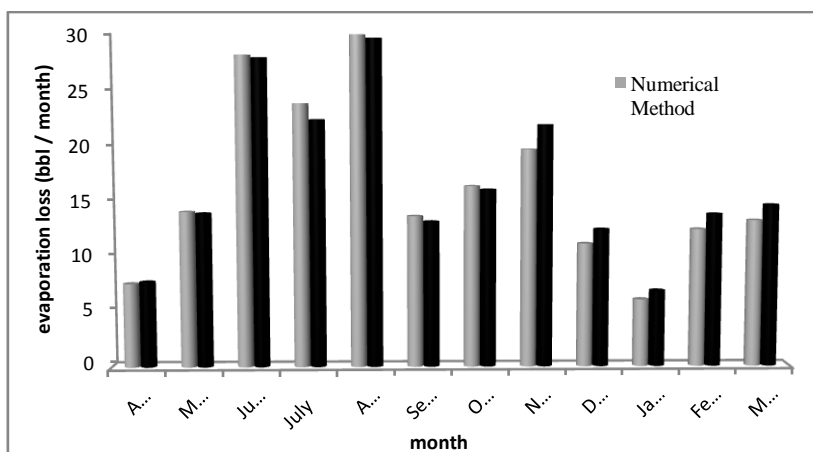


Figure 13 –Comparison of the monthly averaged total evaporative losses



Fig. 14 shows the effects of the paint absorptivity of the storage tank on the monthly averaged evaporative losses throughout the year 2010. As figure indicates, the absorptivity strongly influences the evaporation rate especially during the summer months. The evaporative losses increases by about 300%, when the absorptivity of the paint increases from  $\alpha = 0.1$  to  $\alpha = 0.9$  in August. Note that the evaporative losses in February and December are the same for all absorption coefficients due to the similar solar radiation and wind condition in these months. This is almost the case for the months of July and June.

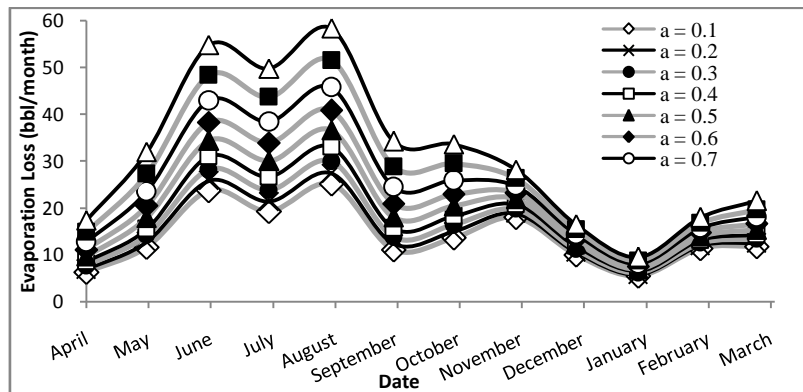


Figure 14 – Surface paint absorptivity effects on monthly variations of the evaporative losses

Annual averaged evaporative losses from the storage tank for different absorption coefficients are shown in Figure 15. A curve is fitted to the numerical values, which is expressed with the following simple expression.

$$Loss(barrel) = 200.7\alpha^2 + 51.59\alpha + 161.9 \quad (32)$$

The results indicate that simply by painting exterior surfaces by clean white ( $\alpha=0.2$ ), the annual evaporative losses reduce by about 20 barrels as compared to the dirty white ( $\alpha=0.3$ ). There are about 200 barrels difference between the light color ( $\alpha=0.1$ ) and the dark color ( $\alpha=0.9$ ) paints for a single storage tank. Since there are about 40 storage tanks in the Khark island total evaporative losses can be considerable. Furthermore, the amount of evaporative losses for lighter hydrocarbons is probably much higher than crude oil which calculated here, therefore, the absorptivity of the exterior surface paint of the storage tanks for such products plays more important roles, which must be considered.

Considering the fact that the evaporation basically occurs in the crude oil layers adjacent to the floating roof, the local temperature in this area is a key factor in this process. Clearly, the insulation of the tank roof, which absorbs the largest portion of the solar irradiation, reduces its temperature and the amount of evaporative losses accordingly.

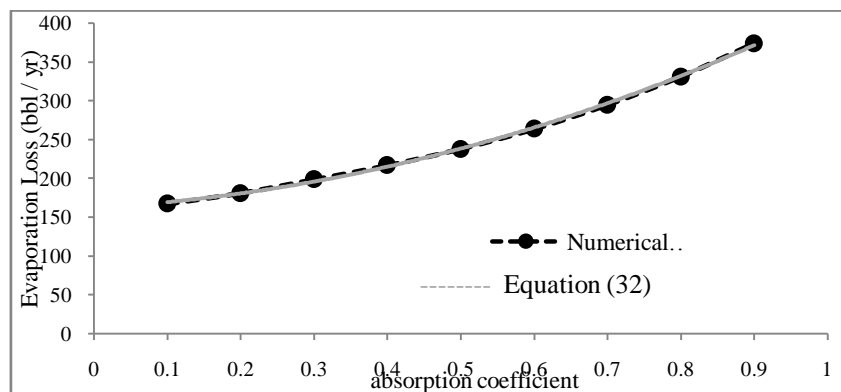


Figure 15- Annual evaporative losses as a function of the surface paint absorption coefficient

## V. CONCLUSIONS

In this study a numerical scheme has been developed for estimating the time variations of the storage tank temperature and evaporative losses. The numerical value of monthly averaged evaporation losses have been compared with the estimations based on the API AP-42 standard. Considering the fact that the evaporation mainly occurs at the fluid surface under floating roof, therefore, surface temperature becomes important parameter. Any mechanisms that reduce the floating roof temperature will directly affect the evaporation rate. Therefore, the exterior surface paint absorptivity and even the cleaning of the floating roof, where dust can accumulate and increase the absorptivity of the surface becomes an issue. Present results indicate that the annual evaporative losses increase up to 125% if the absorptivity of the tank surface increases such that 90 percent of the solar irradiation is absorbed. It is expected that just by insulating the floating tank roof the evaporative losses reduce considerably. Furthermore, the evaporative losses are affected by the wind speed, which will reduce by adding wind shield system especially to the sealing system of the floating roof.

<b>Nomenclature</b>			
$A_s$	Area ( $m^2$ )	$PA$	atmospheric pressure, (kpa)
$A$	constant in the vapor pressure equation, (dimensionless)	$P^*$	vapor pressure function, (dimensionless)
$B$	constant in the vapor pressure equation ( $^{\circ}K$ )	$Pr$	Prandtl Number (dimensionless)
$c_p$	Special heat capacity (J/kg-K)	$PVA$	true vapor pressure, (kpa)
$C_s$	shell factor, (m)	$Q$	annual throughput, ( $m^3/yr$ )
$D$	tank diameter, (m)	$q$	Heat transfer energy ( $W/m^2$ )
$F_c$	effective column diameter, (m)	$q_s$	Absorbed solar energy ( $W/m^2$ )
$F_F$	total deck fitting loss factor, (kg-mole/yr)	$q_{conv}$	Convection Heat transfer energy ( $W/m^2$ )
$H_0$	cloudless daily global irradiation received, ( $MJ/m^2 \cdot hour$ )	$q_{cond}$	Conduction Heat transfer energy ( $W/m^2$ )
$H$	daily global irradiation, ( $MJ/m^2 \cdot hour$ )	$q_{sky}$	Radiation to sky ( $W/m^2$ )
$h$	convection coefficient ( $w/m^2 k$ )	$Ra$	Rayleigh number (dimensionless)
$h_{fg}$	evaporate enthalpy (KJ/kg)	$S$	average sunshine duration, (hour)
$h_{in}$	inlet enthalpy (KJ/kg)	$S_0$	cloudless sunshine duration, (hour)
$h_{out}$	Outlet enthalpy (KJ/kg)	$T_{\infty}$	ambient temperature ( $^{\circ}K$ )
$K$	conductivity ( $W/m K$ )	$TS$	tank surface temperature, ( $^{\circ}K$ )
$K_{Ra}$	zero wind speed rim seal loss factor, ( kg-mole/m@ yr)	$T_{sky}$	Sky temperature ( K)
$K_{Rb}$	wind speed dependent rim seal loss factor, (kg-mole/(m/s) <sup>n</sup> m @yr)	$T_{soil}$	Soil temperature ( K)
$M_v$	vapor molecular weight, (kg/kg-mole)	$U$	Internal energy (j)
$m$	Mass (kg)	$V$	average ambient wind speed, (m/s)
$\dot{m}$	total loss, (kg/s)	$\dot{W}$	Rate of work (W)
$m_F$	deck fitting loss, ( kg/s)	$WL$	average organic liquid density, ( $kg/m^3$ )
$m_R$	rim seal loss, (kg/s)	<b>Greek Symbols</b>	
$m_{WD}$	withdrawal loss, (kg/s)	$\alpha$	Absorption coefficient, (dimensionless)
$\dot{m}_{in}$	Inlet mass (kg/s)	$\delta$	declination angle, (degree)
$\dot{m}_{out}$	Outlet mass (kg/s)	$\varphi$	Longitude, (degree)
$N$	Number of day in year	$\omega$	hour angle, (degree)
$NC$	number of fixed roof support columns, (dimensionless)	$\epsilon$	emissivity (dimensionless)
$Nu$	Nusselt number (dimensionless)	$\sigma$	Stefan–Boltzmann constant ( $W/m^2 K^4$ )

### Reference

- [1] H. K. Abdel-Aal, M. Aggour, M. A. Fahim, Petroleum and gas field processing, In: Chapter 8- Storage Tanks and Other Field Facilities, New York: Marcel Dekker Inc; p. 1 (2003).
- [2] R.J. Laverman, Emission Reduction Options for Floating Roof Tanks, Second International Symposium on Aboveground Storage Tanks, Houston; (1992).
- [3] S. Ramachandran, Reducing (controlling) vapor losses from storage tanks, 7<sup>th</sup> annual India Oil & Gas Review, Symposium & International Exhibition, Bombay, (IORS-2000).
- [4] Ciolek Michael, Emission Factor Documentation for AP-42 Section 7.1 Organic Liquid Storage Tanks, In: Chapter 2- Storage Tank Descriptions, U S Environmental Protection Agency; p.1-5 (2006).
- [5] S. Wongwises, I. Rattanaprayura, S. Chanchaona, An Evaluation of Evaporative Emissions of Gasoline from Storage Sites and Service Stations, Thailand, Thammasat Int. J Sc Tech. Vol 2, No 2, (July 1997).

- [6] H. Asharif, E. Zorgani, Adjustment of Process Variables to Reduce Evaporation Losses from High pour point-crude oil storage tanks, The 8<sup>th</sup> international conference on petroleum phase behavior and fouling, France, 10-14 (June 2007).
- [7] D. Digrado Brian, A. Thorp Gregory, The aboveground steel storage tank handbook, In: chapter 13: new field-erected aboveground storage tank products, New Jersey: John Wiley & Sons Inc; p. 127. (2004).
- [8] Evaporative Loss from External Floating Roof Tanks, Bulletin No. 2517, Third Edition, American Petroleum Institute, Washington, DC, (1989).
- [9] Evaporative Loss from Internal Floating Roof Tanks, API Publication 2519, American Petroleum Institute, Washington, DC, (March 1990).
- [10] S. Zareie, D. Mowla, J. Fathi, Practical Study of VOCs Emission from External Floating Roof Tanks, 5th international congress of chemical engineering, Shiraz, Iran; (2007).
- [11] Wang Xiaoxin, Kendrick Chris, Ogden Ray, Maxted James, Dynamic thermal simulation of a retail shed with solar reflective coatings. Thermal Engineering 1073-1066. (2008);
- [12] ekai, Sen, Solar Energy Fundamentals and Modeling Techniques, Londen: Springer Veriag. p. 47-140. (2008).
- [13] G. A. Kamali, E. Moradi, Solar radiation fundamentals and application in farms and new energy, Tehran: publication 21 century; (2005).
- [14] S. W. Churchill, M. A. Bernstein, Correlating Equation for Forced Convection from Gases and Liquids to a Circular Cylinder in Cross Flow, J Heat Transfer. 300-306. (1977);
- [15] Manual of Petroleum Measurement Standards, In: Chapter 19- Evaporative Loss Measurement, Section 2- Evaporative Loss From Floating Roof Tanks. Preliminary Draft, American Petroleum Institute, Washington DC; (1994).
- [16] Ciolek Michael, Emission Factor Documentation for AP-42 Section 7.1 Organic Liquid Storage Tanks. In: Chapter 3-Emission Estimation Procedure. U S Environmental Protection Agency; p. 9-11: 15-18. (2006).